Microscale, High-Precision Si-Isotope Analyses with the IMS-1280 Ion Microprobe

Heck P.R.*, Kita N.T., Johnson C.M., Valley J.W.
University of Wisconsin, Madison, Department of Geology & Geophysics, *prheck@geology.wisc.edu

Wisconsin Astrobiology Research Consortium

Introduction

The Si isotopic compositions of terrestrial materials range from –7.5‰ in macrocrystalline quartz of groundwater silcretes (Basile-Doelsch et al. 2005) to +6.1‰ in opaline silica of rice grains (Ding et al. 2005). Si isotopes have been used to study the biogeochemical cycle of Si in the ocean (De La Rocha et al. 2005) and on the continents (Basile-Doelsch et al. 2005). Biogenic precipitation of silica as well as weathering and silicification are the major players in the terrestrial Si cycle.

Si isotopes appear to be very robust and retain primary isotopic compositions even during metamorphism (André et al. 2006).

Si in conjunction with isotopes of O, Fe, S and C have the potential to constrain formation conditions and origins of rocks and soils, and link them to biosignatures.

The development of high-precision isotope analyses with the IMS-1280 allows us to measure different isotope systems *in situ* on the identical mineral grain and allows us to analyze small domains in contrast to mixed or bulk signals obtained by other techniques.

Sample preparation

The sample and standards are mounted within 5 mm of the center of a flat 1-inch mount. The mount is ground and polished in order to minimize surface relief. High relief reduces the precision and accuracy of SIMS measurements.

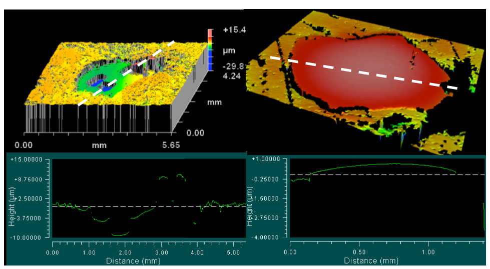

Fig.1. White light profilometer 3D visualization of top-mounted UWQ-1 quartz (both panels: red, elevated) and UWC-3 calcite (left panel: blue, depressed) standard grains on Precambrian BIF samples. The different hardness of the minerals ($H_{Qtz.}$=7 vs. $H_{Cc.}$=3) make it difficult to obtain a flat surface by grinding/polishing and result in uneven relief (left panel). The use of diamond lapping films reduces the amount of relief to a minimum as shown on the right panel.

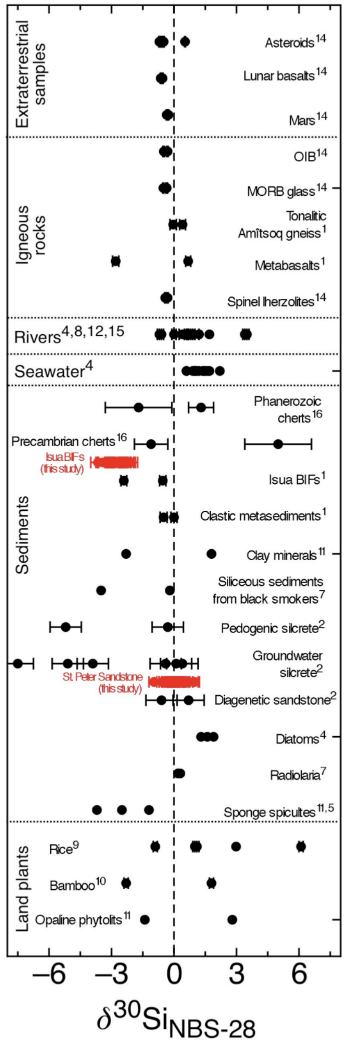

Fig.2. δ^{30}Si of selected natural samples (2σ errors). The most extreme δ^{30}Si values besides circumstellar minerals are observed to occur in silcretes, hydrothermal siliceous sediments, sponge spicules and rice grains. Superscript numbers refer to published data of which extreme and average data are shown.

Goals

We are developing Si isotope standards for various minerals.

In a systematic study we will test the effect of metamorphism on Si isotope compostion in quartz in the Biwabik banded iron formation (BIF) in Minnesota which has been studied already for Fe and O isotopes (Valaas Hyslop et al. 2008).

We will analyze Si-isotopes on the 10 micron, sub-mineral scale and will compare them with O, C, S and Fe isotopes of the same locations in BIFs from different times and continents (Isua 3.8 Ga, Hamersley and Transvaal 2.5 Ga, Biwabik 1.9 Ga).

The origin of rocks and soils, with biosignatures detected with Fe, C and S isotopes will be constrained by the Si isotopic composition. Formation conditions can be further assessed by correlation of Si with O isotopes.

Si Isotope Standard Developments

Standard analyses are used to bracket sample analyses. Quartz and garnet standards (UWQ-1 & UWG-2) were calibrated by ICP-MS (Georg 2006):

δ^{30}Si = –0.03 ± 0.04 ‰ (UWQ-1)
δ^{30}Si = 0.29 ± 0.04 ‰ (UWG-2)

Opal and zircon standards are in development.

Testing the isotopic homogeneity of standards on the micron scale at sub-‰ precision (WiscSIMS IMS-1280):

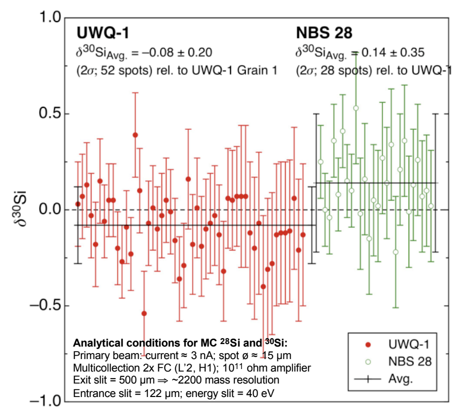

Fig.3. δ^{30}Si measurements on a polished quartz standard grain mount with UWQ-1 and NBS-28 grains. A primary Cs^+ beam of ~3 nA and a spot diameter of ~ 15 µm resulted in a precision of 0.2 ‰ (2σ) on UWQ-1.

Preliminary Results

Si-isotope ion microprobe analyses of individual quartz minerals in Archean banded iron formation rocks from Isua, Greenland with a ~15 µm Cs^+ beam of ~3 nA .

δ^{30}Si of quartz in quartz-rich layers has a larger variation (–3.7‰ to –2.1‰) than in magnetite-rich layers (–3.0‰ to –2.3‰), the precision is 0.3‰ to 0.4‰ (2σ). Our preliminary data extend the range of δ^{30}Si in BIFs by >1‰ and confirm recent 500 µm-scale MC-ICP-MS analyses by André et al. (2006) and hence provides further evidence that the BIF quartz is a hydrothermal fluid precipitate similar to modern-day siliceous sea-floor sediments associated with black smokers.

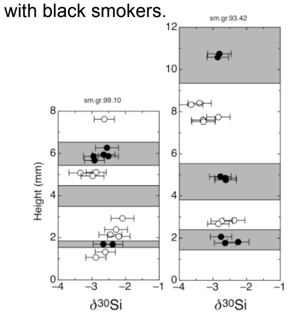

Fig.4. δ^{30}Si of quartz in magnetite-rich layers (black symbols) and quartz-rich layers (white symbols) of two BIF samples from Isua, Greenland. Errors are based on the bracketing standard UWQ-1 and are 0.3 to 0.4‰ (2σ).

δ^{30}Si of Ordovician St. Peter sandstone range from –1.0‰ to +1.6‰. In our preliminary study of three samples no clear trend in δ^{30}Si of detrital quartz cores vs. quartz overgrowth has been observed.

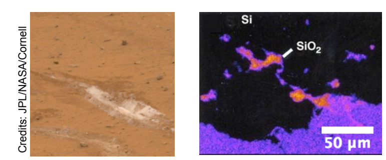

Fig.5. (A) Silica-rich material discovered by the rover Spirit in Gusev Crater in a 20-cm-wide track of disturbed martian soil. (B) Silica in an electron microprobe Si image of martian meteorite ALH84001 (Valley et al. 1997). Silica associated with past hydrothermal activity would be well suited to look for isotopic biosignatures on Mars (Squyres et al. 2008).

Acknowledgements: We thank B. Hess for help with sample preparation, J. Fournelle for help with SEM/EDS and J. Kern and R. Kozdon for support with SIMS analyses. We thank S. Moorbarth, C. Klein and R. Dymek for the Isua sample collection and J. Kelly for the St. Peter sandstone.

References

[1] André L. et al. (2006) *EPSL* 245, 162. [2] Basile-Doelsch I. et al. (2005) *Nature* 433, 399. [3] De La Rocha et al. (1998) *Nature* 395, 680.[4] De La Rocha et al. (2000) *GCA* 64, 2467. [5] De La Rocha et al. (2003) *Geology* 31, 423. [6] De La Rocha et al. (2005) *Marine Geology* 217, 267. [7] Ding et al. (1996) *Silicon Isotope Geochemistry*. [8] Ding et al. (2004) GCA 68, 205. [9] Ding et al. (2005) *Chem. Geo.* 218, 41. [10] Ding et al. (2008) *GCA* 72, 1381. [11] Douthitt C.B. (1982) *GCA* 46, 1449. [12] Gao et al. (2006) *GCA* 70, A192. [13] Georg B. (2006) Ph.D. Thesis, ETH Zürich. [14] Georg B. et al. (2007) *Nature* 447, 1106. [15] Reynolds B.C. (2006) *GCA* 70, A530. [16] Robert F. & Chaussidon M. (2006) *Nature* 443, 969. [17] Squyres S.W. et al. (2008) *Science* 320, 1063. [18] Valaas Hyslop et al. (2008) *Contrib. Mineral. Petrol.* 155, 313. [19] Valley et al. (1997) *Science* 275, 1633.